

Structure of the neutron mid-shell nuclei $^{111,113}_{47}\text{Ag}_{64,66}$

S. Lalkovski^{1*}, E. A. Stefanova², S. Kisyov³, A. Korichi⁴, D. Bazzacco⁵, M. Bergström⁶,
 A. Görgen⁷, B. Herskind⁶, H. Hübel⁸, A. Jansen⁸, T.L. Khoo⁹, T. Kutsarova²,
 A. Lopez-Martens⁴, A. Minkova¹, Zs. Podolyák¹⁰, G. Schönwasser⁸, O. Yordanov²

¹*Department of Nuclear Engineering, Faculty of Physics,
 University of Sofia "St. Kl. Ohridski", Sofia 1164, Bulgaria*

²*Institute for Nuclear Research and Nuclear Energy,
 Bulgarian Academy of Science, Sofia 1784, Bulgaria*

³*"Horia Hulubei" National Institute for Physics and Nuclear Engineering,
 RO-077125 Bucharest, Romania*

⁴*CSNSM Orsay, IN2P3/CNRS, F-91405, France*

⁵*INFN, Sezione di Padova, I-35131 Padova, Italy*

⁶*The Niels Bohr Institut, Blegdamsvej 17,
 DK-2100 Copenhagen, Denmark*

⁷*Department of Physics,
 Faculty of Mathematics and Natural Sciences,
 University of Oslo, Norway*

⁸*Helmholtz-Institut für Strahlen -und Kernphysik,
 Universität Bonn, Nussallee 14-16,
 D-53115 Bonn, Germany*

⁹*Physics Division, Argonne National Laboratory,
 Argonne, Illinois 60439, USA*

¹⁰*Department of Physics,
 University of Surrey, Guildford GU27XH, UK*

(Dated: October 20, 2018)

^{111}Ag and ^{113}Ag were produced in induced fission reaction, where yrast and near-yrast states were populated. To interpret the new data the Interacting Boson-Fermion model was used. A good agreement with the experimental data is achieved, suggesting that the two Ag nuclei have a well developed collectivity, superimposed on $\pi g_{9/2}^{-3}$ excitations previously observed throughout the entire isotopic chain.

PACS numbers: 21.10.-k, 21.10.Re, 21.60.Ev, 23.20.Lv, 27.60.+j

I. INTRODUCTION

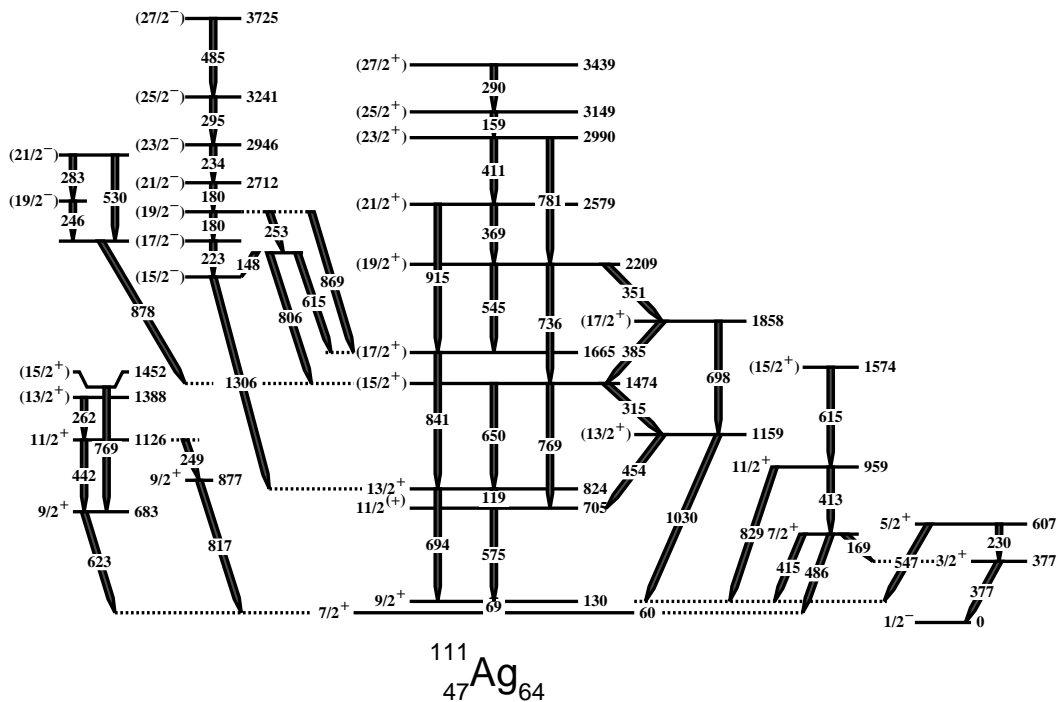
Silver nuclei present an excellent ground for testing of different theoretical models. Being three proton holes away from the Sn nuclei, they represent a good test case for the Nuclear Shell model [1]. Indeed, the $j-1$ anomaly, observed in the low-energy part of Ag spectra, is often interpreted as arising from three-hole clusters [2] – a direct derivative from the Shell model [3]. Within that approach, however, the $M1$ transitions between members of the same multiplet are forbidden [4] which, to certain extent, coincides with the experimental observation [5]. Detailed shell model calculations [6], however, seem to fail in describing those states. Neither their ordering, nor the $(j, j-1)$ energy gap is well reproduced, which was assumed to arise from enhanced $p-n$ interaction.

Attempts to explain the structure of the low-lying states in Ag nuclei were also made in the framework of different collective and algebraic models [7]. Indeed, already in the early 60's de-Shalit [8] demonstrated that

the low-lying negative-parity states in Ag isotopes represent core excitations, weakly coupled to the odd unpaired particle. These studies were followed by the Cluster-Vibration model developed [9] and applied for an extensive set of levels in the Ag nuclei. Quasi-particle-plus rotor model calculations were performed in Refs. [10, 11] and Interacting Boson-Fermion Model calculations in Ref. [12, 13]. It was pointed out [7] that, in addition to magnetic moments and electromagnetic transition strengths, a reasonable explanation of the $j-1$ anomaly can be achieved by using enhanced quadrupole residual interaction.

Although the neutron mid-shell Ag nuclei are of paramount importance for testing of various models, the experimental data is often scarce. In particular, little is known about the yrast states in the mid-shell ^{111}Ag [14] and ^{113}Ag [15]. To fill in the gap, we report on new data from induced fission reaction. The extended level schemes are analyzed by using IBFM-1 calculations.

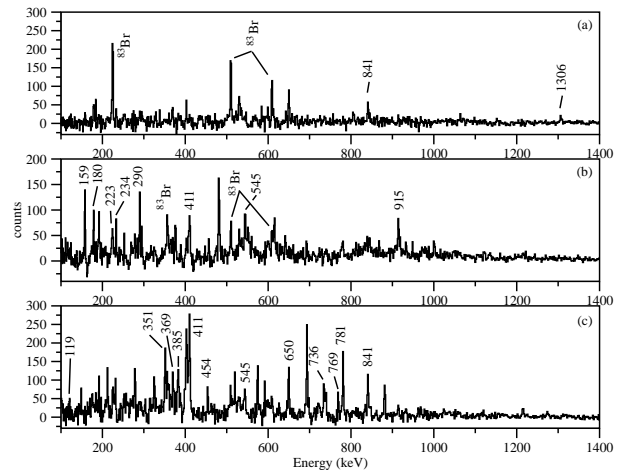
*e-mail: stl@phys.uni-sofia.bg

FIG. 1: ^{111}Ag partial level scheme.

II. EXPERIMENTAL DETAILS

$^{111,113}\text{Ag}$ were produced in induced fission reaction. The $^{30}_{14}\text{Si}$ beam was accelerated up to $E = 142$ MeV by the XTU tandem accelerator at the Legnaro National Laboratory, and impinged on a 1.15 mg/cm 2 thick ^{168}Er target. To stop the recoil fission fragments, the target was deposited on a 9 mg/cm 2 gold backing. Gamma-rays, emitted from the excited nuclei, were detected by the EUROBALL III multi-detector array [16], comprising 30 single HPGe detectors, 26 Clover and 15 Cluster detectors with anti-Compton shields. Triple γ ray coincidences were recorded. The data was sorted in $E_\gamma - E_\gamma - E_\gamma$ cubes and analyzed by using the RADWARE software [17].

The compound nucleus, produced in this reaction, is $^{198}_{72}\text{Pt}$. The dominant reaction channel is the fusion/evaporation reaction leading to $^{194,195}_{82}\text{Pb}$ [18]. The induced fission reaction represents only a small fraction of the total cross section. In such reactions, the proton evaporation is highly suppressed and the sum of the fragments' atomic numbers is equal to the atomic number of the fissioning system. Hence, the most populated complementary fragments of ^{111}Ag and ^{113}Ag are $^{83}_{35}\text{Br}$ and $^{81}_{35}\text{Br}$, respectively. More details about this experiment, and other fission products produced in it, are published in Refs. [19–21].

FIG. 2: Sample coincidence spectra for ^{111}Ag , gated on 356-keV γ ray in ^{83}Br and 694-keV γ ray in ^{111}Ag (a), and on 694- and 841-keV γ rays (b), and 290- and 159-keV γ rays (c), respectively.

A. ^{111}Ag

The partial level scheme, obtained from cross coincidences between ^{111}Ag and its complementary fragment ^{83}Br , is presented in Fig. 1. Once coincident transitions are established to belong to ^{111}Ag , they were used to further extend the level scheme. The procedure used in the present work is similar to the one used to build the positive-parity bands placed on top of the ground states of $^{107,109}\text{Pd}$ [20] and ^{105}Ru [21]. Sample coinci-

TABLE I: Data set of ^{111}Ag levels and γ -rays as observed in the present work, but also known from the literature [14]. Level energies, E_i and E_f in keV, are obtained after a least-squares fit to the energies of the γ rays E_γ connecting the respective initial and final states. BR_γ are the gamma-decay branching ratios. With few exceptions discussed in the text, the spin/parity assignments J^π are from Ref. [14].

E_i	J_i^π	E_f	J_f^π	E_γ	BR_γ
0	$1/2^-$				
60.1	$7/2^+$				
129.6	$9/2^+$	60.1	$7/2^+$	68.8	
376.6	$3/2^+$	0	$1/2^-$	376.6	
545.4	$7/2^+$	376.6	$3/2^+$	168.9	23 (2)
		129.6	$9/2^+$	415.4	100
		60.1	$7/2^+$	486.0	16 (2)
607.0	$5/2^+$	376.6	$3/2^+$	230.3	
		60.1	$7/2^+$	547.0	
683.3	$9/2^+$	60.1	$7/2^+$	623.3	
704.9	$11/2^{(+)}$	129.6	$9/2^+$	575.2	
823.9	$13/2^+$	704.9	$11/2^{(+)}$	118.9	< 5
		129.6	$9/2^+$	694.3	100
876.9	$9/2^+$	60.1	$7/2^+$	816.8	
958.5	$11/2^+$	544.4	$7/2^+$	413.3	
		129.6	$9/2^+$	828.7	
1125.7	$11/2^+$	876.9	$9/2^+$	248.7	
		683.3	$9/2^+$	442.4	
1159.4	$(13/2^+)$	704.9	$11/2^{(+)}$	454.2	
		129.6	$9/2^+$	1030.0	
1388.3	$(13/2^+)$	1125.7	$11/2^+$	262.6	
1452.1	$(15/2^+)$	683.3	$9/2^+$	768.8	
1474.0	$(15/2^+)$	1159.4	$(13/2^+)$	314.8	12 (2)
		823.9	$13/2^+$	650.3	100
		704.9	$11/2^{(+)}$	769.4	55 (4)
1573.6	$(15/2^+)$	958.5	$11/2^+$	615.1	
1664.5	$(17/2^+)$	823.9	$13/2^+$	840.9	
2130.6	$(15/2^-)$	823.9	$13/2^+$	1306.1	
2352.8	$(17/2^-)$	2130.6	$(15/2^-)$	222.6	
		1474.0	$(15/2^+)$	878.4	

dence spectra for ^{111}Ag are shown in Fig. 2. Gamma-ray energies E_γ and branching ratios BR_γ are listed in Table I and II along with energies of the initial E_i and final E_f states, obtained from a least-squares fit to E_γ . Table I presents the levels known prior to our study. Indeed, ^{111}Ag [14] was previously studied from ^{111}Pd β^- decay [22], $^{109}\text{Ag}(t,p)$ [23], $^{110}\text{Pd}(^3\text{He},d)$ [24], $^{110}\text{Pd}(^3\text{He},pn\gamma)$ [25], and $^{112}\text{Cd}(d,^3\text{He})$ [26] reactions. In addition to the levels presented in Table I many other non-yrast positive and negative parity were previously observed [14]. Table II lists the levels and gamma-rays observed for the first time in the present work.

Due to the poor statistics in the present study no angular correlation nor angular distribution measurements were performed. Therefore, the spin and parities in the present work are based on: the spin and parities already assigned in Refs. [14, 15]; the analogy with ^{107}Ag , where angular correlation measurements were performed; and on the systematics [6]. The new transitions are assumed

TABLE II: Data set of ^{111}Ag levels and gamma rays observed for the first time in the present study. Continues from Table I.

E_i	J_i^π	E_f	J_f^π	E_γ	BR_γ
1858.2	$(17/2^+)$	1474.0	$(15/2^+)$	384.6	100
		1159.4	$(13/2^+)$	698.3	55 (7)
2209.4	$(19/2^+)$	1858.2	$(17/2^+)$	351.1	60 (5)
		1664.5	$(17/2^+)$	544.5	78 (6)
		1474.0	$(15/2^+)$	735.6	100
2279.9	$(17/2^+)$	2130.6	$(15/2^-)$	148.1	70 (3)
		1664.5	$(17/2^+)$	615.0	100
		1474.0	$(15/2^+)$	806.4	38 (3)
2532.7	$(19/2^-)$	2352.8	$(17/2^-)$	179.8	
		2279.9	$(17/2^+)$	252.7	
		1664.5	$(17/2^+)$	868.7	
2579.2	$(21/2^+)$	2209.4	$(19/2^+)$	369.2	13 (2)
		1664.5	$(17/2^+)$	914.9	100
2599.1	$(19/2^+)$	2352.8	$(17/2^-)$	246.1	
2712.3	$(21/2^-)$	2532.7	$(19/2^-)$	179.6	
2882.6	$(21/2^+)$	2599.1	$(19/2^+)$	283.3	
		2352.8	$(17/2^-)$	530	
2946.0	$(23/2^-)$	2712.3	$(21/2^-)$	233.7	
2990.1	$(23/2^+)$	2579.2	$(21/2^+)$	410.5	100
		2209.4	$(19/2^+)$	781.1	79 (4)
3148.9	$(25/2^+)$	2990.1	$(23/2^+)$	158.8	
3240.9	$(25/2^-)$	2946.0	$(23/2^-)$	294.9	
3438.7	$(27/2^+)$	3148.9	$(25/2^+)$	289.8	
3725	$(27/2^-)$	3241	$(25/2^-)$	484.5	

to be of dipole and quadrupole multipolarity only.

In Ref. [14], based on reaction data and angular distribution measurements, spin and parity assignments have been made to all states below the 1574-keV state. In contrast to [14] where $(11/2)$ is assigned to the 1388-keV level we tentatively assign $(13/2^+)$ assuming that in the induced fission experiments spins increase with the energy. Based on the same argument the spin/parity assignments were made to the 1159-, 1452-keV levels. The spin/parity assignments to the 1474-, 1665-keV levels are also based on the afore mentioned argument and the systematics. The structure built of low energy transitions on top of the 2131-keV state, is similar to the structure observed on top of the 2298-keV state in ^{107}Ag . In ^{111}Ag , as in ^{107}Ag , the sequence decays to the yrast $13/2^+$ state via 1.3-MeV transition. Therefore, we tentatively assume this sequence to be a $\Delta I = 1$ band of negative-parity states.

The sequence, built on top of the $7/2^+$ state at 60 keV, is extended up to 3439 keV. This band-like structure resembles the sequence observed in ^{107}Ag [27] and is consistent with the systematic trend of the low-lying positive-parity yrast states in the Ag isotopic chain [6].

B. ^{113}Ag

^{113}Ag [15] was studied previously via β^- decay of ^{113}Pd . Many low-spin states of positive and negative

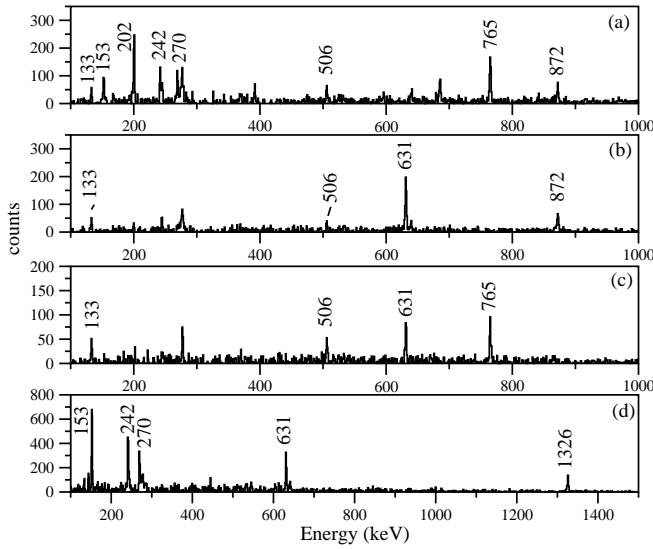


FIG. 3: Sample coincidence spectra for ^{113}Ag , representing the 95γ - 631γ (a), 95γ - 765γ (b), 95γ - 872γ (c), and 202γ - 201γ coincidences (d).

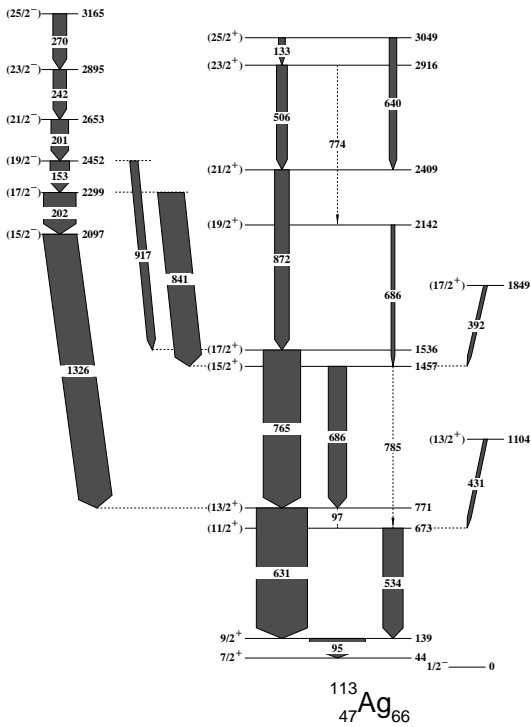


FIG. 4: ^{113}Ag partial level scheme.

parities were observed, but the level scheme is incomplete given that $Q_{\beta^-} = 3.4$ MeV and only levels up to 0.783 MeV were experimentally observed.

Being further away from the line of β^- -stability than ^{111}Ag , ^{113}Ag is difficult to populate via light particle transfer reactions and fusion/evaporation reactions. Also, it is not well produced in spontaneous fission. Thus,

TABLE III: Data set of ^{113}Ag levels and gamma rays as observed in the present work. Level energies E_i and E_f are obtained after a least-squares fit to the γ -ray energies E_γ in keV. Relative γ ray intensities (I_γ) are normalized to $I_{765} = 100\%$. Except for the levels, denoted with an a symbols which were known prior to this study [15], the spin/parity assignments J^π to the rest of the levels are from this work.

E_i	J_i^π	E_f	J_f^π	E_γ	I_γ
0^a	$1/2^-$				
44^a	$7/2^+$				
139.1 a	$9/2^+$	44	$7/2^+$	95.1	94
673.1 a	$(11/2^+)$	139.1	$9/2^+$	534.2	54
770.7	$(13/2^+)$	139.1	$9/2^+$	631.4	137
		673.1	$(11/2^+)$	97.1	39
1104.1	$(13/2^+)$	673.1	$(11/2^+)$	431	
1457.0	$(15/2^+)$	770.7	$(13/2^+)$	685.6	49
		673.1	$(11/2^+)$	784.6	20
1536.0	$(17/2^+)$	770.7	$(13/2^+)$	765.3	100
1849.0	$(17/2^+)$	1457.0	$(15/2^+)$	392	
2096.8	$(15/2^-)$	770.7	$(13/2^+)$	1326.0	104
2142.3	$(19/2^+)$	1457.0	$(15/2^+)$	686	
2298.8	$(17/2^-)$	2096.8	$(15/2^-)$	202	87
		1457.0	$(15/2^+)$	841.2	71
2408.7	$(21/2^+)$	1536.0	$(17/2^+)$	872.1	39
2452.1	$(19/2^-)$	2298.8	$(17/2^-)$	152.6	52
		1457.0	$(15/2^+)$	916.8	22
2652.7	$(21/2^-)$	2452.1	$(19/2^-)$	200.6	47
2894.9	$(23/2^-)$	2652.7	$(21/2^-)$	242.2	29
2915.7	$(23/2^+)$	2408.7	$(21/2^+)$	506.2	29
3049.0	$(25/2^+)$	2915.7	$(23/2^+)$	133.2	18
		2408.7	$(21/2^+)$	640.4	20
3164.5	$(25/2^-)$	2894.9	$(23/2^-)$	269.6	36

the experiment described in the present work opens a new opportunity to study this particular nucleus, given that the fissioning ^{198}Pb system is lighter than any of the spontaneous fissioning sources traditionally used to populate nuclei on the neutron-rich side of the β^- stability line.

In all complementary Br fragments, lines with energies of 95, 631 and 534 keV were observed. The 95- and 534-keV lines were known to belong to ^{113}Ag [15]. They were used in the present work to identify the most populated complementary fragment of ^{113}Ag , which is ^{81}Br . Coincidences between these 631- and 534-keV transitions and the most intense transitions in ^{81}Br were analysed to deduce the other yrast states in ^{113}Ag . The higher lying states in ^{113}Ag were established from coincidences with the most intense transitions already assigned to ^{113}Ag . Sample coincidence spectra are displayed in Fig. 3 and the new level scheme is shown in Fig. 4.

It has to be noted, that the 431-keV transition is also in coincidence with the transitions from the sequence on top of the 2097-keV level. However, no link between the two structures was observed, suggesting that the 2097-keV level decays via multiple weak transitions to several intermediate states.

The spin and parity assignments to the levels are based

on the values adopted in Ref. [15] for the lowest-lying states, on systematics [6], and on analogy with the ^{115}Ag level scheme. Again, only dipole and quadrupole type of transitions are assumed.

III. DISCUSSION

A. IBM-1 calculations

To interpret the new data, Interacting Boson-Fermion Model (IBFM) [28, 29] calculations were performed for $^{111,113}\text{Ag}$. The model describes the excited states of odd-A nuclei via a coupling of the last unpaired fermion to the even-even bosonic core. In the present work, the cadmium nuclei $^{112,114}\text{Cd}$ are considered to be the even-even cores of $^{111,113}\text{Ag}$. Core excited states were calculated by using the IBM-1 model [30–33] within its extended consistent- Q formalism (ECQF) [34, 35], where the model Hamiltonian can be written as

$$H = \varepsilon n_d - \kappa Q^2 - \kappa' L^2. \quad (1)$$

Here,

$$n_d = \sqrt{5}T_0$$

is the number of d -bosons operator. The total number of bosons $N = n_s + n_d$ is then taken as half the number of valence particles or holes, counted from the nearest closed-shell gap [36]. This version of the IBM does not distinguish protons from neutrons.

In IBM-1, the angular momentum operator is defined as

$$L = \sqrt{10}T_1$$

and the quadrupole operator as

$$Q = (d^\dagger s + s^\dagger \tilde{d}) + \chi(d^\dagger \tilde{d})^{(2)} = (d^\dagger s + s^\dagger \tilde{d}) + \chi T_2,$$

where

$$\tilde{d}_\mu = (-1)^\mu d_{-\mu}$$

The eigen states and eigen values were calculated with the program package PHINT [37]. The model parameters, obtained from a fit to experimental data, are summarized in Table IV. Experimental level energies and $B(E2)$ values were used for the purpose of the fit. $^{112,114}\text{Cd}$'s theoretical and experimental level schemes are compared in Fig. 5.

The explicit form of the $E2$ transition operator is

$$T(E2) = e_B[(s^\dagger \tilde{d} + d^\dagger s) + \chi(d^\dagger \tilde{d})^{(2)}] = e_B Q, \quad (2)$$

where e_B is the effective bosonic charge. The reduced transition probabilities are then calculated as

$$B(E2; J_i \rightarrow J_f) = \frac{1}{2J_i + 1} \langle J_f || T(E2) || J_i \rangle^2. \quad (3)$$

TABLE IV: IBM-1 parameters for $^{112,114}\text{Cd}$.

Isotope	ε	κ	κ'	χ
^{112}Cd	0.66	0.0065	-0.005	-0.089
^{114}Cd	0.63	0.0075	-0.005	-0.089

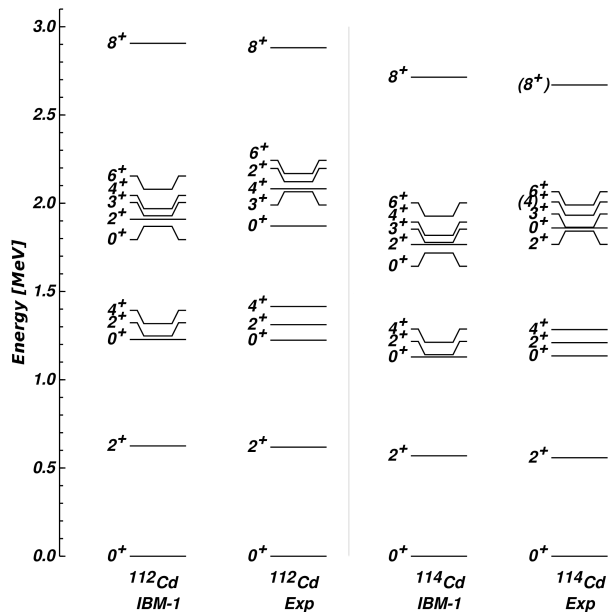


FIG. 5: Theoretical and experimental partial level schemes of $^{112,114}\text{Cd}$. The experimental data are taken from [38].

Here, J_i and J_f denote the spins of the initial and final state, respectively. The effective bosonic charge $e_B = 0.103$ eb is adopted. It is determined from the experimental $B(E2)$ value for the $2_1^+ \rightarrow 0_1^+$ transition in ^{112}Cd . Theoretical and experimental transition probabilities for several low-lying transitions in $^{112,114}\text{Cd}$ are presented in Table V. A good overall agreement with the experimental data is achieved.

B. IBFM-1 calculations

After obtaining the core eigen states, the excited states in $^{111,113}\text{Ag}$ were calculated within the IBFM-1 model, where the Hamiltonian can be written as:

$$H = H_B + H_F + V_{BF}, \quad (4)$$

where H_B is the IBM-1 bosonic Hamiltonian of the even-even core, while the fermionic part of the Hamiltonian is

$$H_F = \sum_j E_j n_j. \quad (5)$$

Here, E_j denotes the quasiparticle energies of the single-particle shell model orbitals.

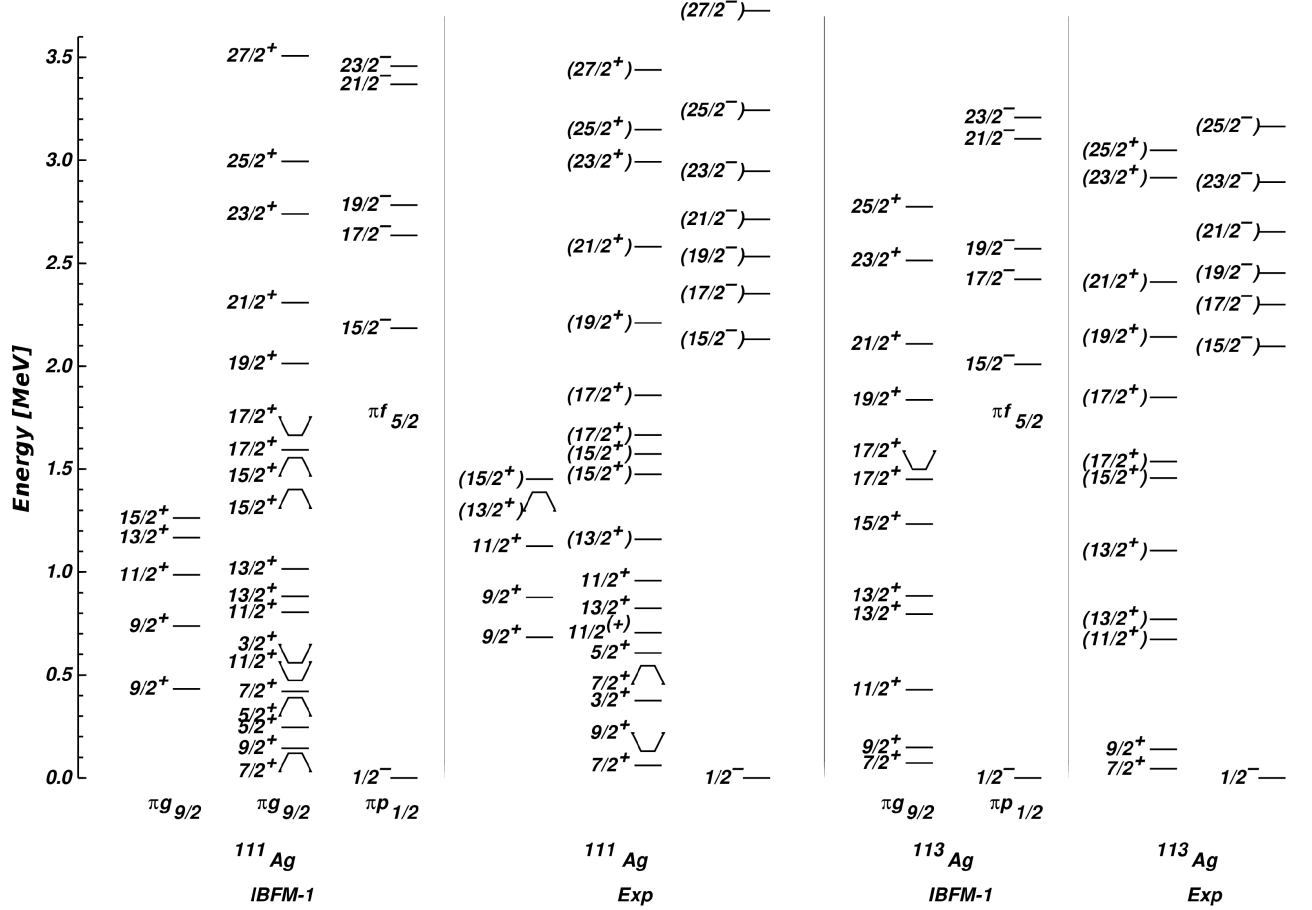


FIG. 6: Partial experimental and theoretical levels in $^{111,113}\text{Ag}$. Each sequence of states has the same leading single-particle component obtained from the IBFM-1 calculations. The model calculations provide information about many other states. A good agreement with the experimental counterparts of those states was observed.

In eq. 4, the term

$$V_{BF} = \sum_j A_j n_d n_j + \sum_{jj'} \Gamma_{jj'} (Q \cdot (a_j^\dagger \tilde{a}_{j'})^{(2)}) + \sum_{jj'j''} \Lambda_{jj'j''} : ((d^\dagger \tilde{a}_j)^{(j'')} \times (\tilde{d} a_{j'}^\dagger)^{(j'')})_0^{(0)} : \quad (6)$$

represents the boson-fermion interaction [28, 39]. This interaction has indeed a large set of parameters which, by using microscopic arguments [40], can be further reduced to

$$A_j = A_0, \\ \Gamma_{jj'} = \Gamma_0 (u_j u_{j'} - v_j v_{j'}) \langle j \parallel Y^{(2)} \parallel j' \rangle, \\ \Lambda_{jj'j''} = -2\sqrt{5}\Lambda_0 \beta_{jj''} \beta_{j''j'} / (2j'' + 1)^{1/2} (E_j + E_{j''} - \hbar\omega). \quad (7)$$

Here,

$$\beta_{jj'} = \langle j \parallel Y^{(2)} \parallel j' \rangle (u_j v_{j'} + v_j u_{j'}), \\ u_j^2 = 1 - v_j^2, \quad (8)$$

and v_j^2 are the occupation probability numbers for the single-particle orbits j . Thus, A_0 , Λ_0 and Γ_0 remain the only free parameters.

The excited states in $^{111,113}\text{Ag}$ were calculated by using the program package ODDA [41]. The single-particle energies were calculated according to the approach described in Ref. [42]. Then, they were applied to the BCS calculation in order to determine the respective occupation probabilities and quasiparticle energies, given in Table VI. The pairing gap was set to $\Delta = 1.5$ MeV.

In the present work, the same set of boson-fermion interaction parameters $A_0 = -0.3$ MeV, $\Gamma_0 = 0.2$ MeV, and $\Lambda_0 = 3.8$ MeV², was used to derive both the positive- and the negative-parity states in the two nuclei. The energy spectra, calculated for $^{111,113}\text{Ag}$ are compared to their experimental counterparts in Fig. 6. The sets of levels having the same leading single-particle component are organized in labeled sequences.

In addition to the level energies, $M1$ and $E2$ transitions probabilities were also calculated and compared to existing experimental data. In IBFM-1, the explicit form

TABLE V: Theoretical and experimental $B(E2)$ values for transitions connecting several normal-parity states in $^{112,114}\text{Cd}$. The experimental data are taken from [38].

Isotope	E_{level} [keV]	J_i^π	E_γ [keV]	J_f^π	$B(E2)_{exp}$ [W.u.]	$B(E2)_{th}$ [W.u.]
^{112}Cd	617.518	2^+	617.518	0^+	30.31 (19)	30.54
^{112}Cd	1224.341	0^+	606.821	2^+	51 (14)	46
^{112}Cd	1312.390	2^+	694.872	2^+	39 (7)	52
			1312.36	0^+	0.65 (11)	0.001
^{112}Cd	1415.480	4^+	798.04	2^+	63 (8)	52
^{114}Cd	558.456	2^+	558.456	0^+	31.1 (19)	35.7
^{114}Cd	1134.532	0^+	576.069	2^+	27.4 (17)	52
^{114}Cd	1209.708	2^+	651.256	2^+	22 (6)	61
			1209.713	0^+	0.48 (6)	0.001
			75.177	0^+	3.4 (7)	0.07
^{114}Cd	1283.739	4^+	725.298	2^+	62 (4)	61
^{114}Cd	1990.3	6^+	706.6	4^+	119 (15)	78
^{114}Cd	2669.3	8^+	678.2	6^+	85 (25)	86

TABLE VI: BCS values for the occupation probabilities v_j^2 and quasiparticle energies E_j of the orbitals. The same set of parameters is used for the two nuclei.

	ϵ_j [MeV]	v_j^2	E_j
$\pi p_{3/2}$	0.0	0.94	3.14
$\pi f_{5/2}$	0.4	0.92	2.80
$\pi p_{1/2}$	1.9	0.75	1.73
$\pi g_{9/2}$	1.8	0.77	1.78
$\pi d_{5/2}$	5.0	0.08	2.69

of the $M1$ and $E2$ operators is:

$$\begin{aligned}
 T(M1) = & \sqrt{\frac{90}{4\pi}} g_d (d^\dagger \tilde{d})^{(1)} \\
 & - g_F \sum_{jj'} (u_j u_{j'} + v_j v_{j'}) \cdot \langle j || g_l l + g_s s || j' \rangle \\
 & \times [(a_j^\dagger \tilde{a}_{j'})^{(1)} + c.c.],
 \end{aligned} \quad (9)$$

$$\begin{aligned}
 T(E2) = & e_B ((s^\dagger \tilde{d} + d^\dagger s)^{(2)} + \chi (d^\dagger \tilde{d})^{(2)}) \\
 & - e_F \sum_{jj'} (u_j u_{j'} - v_j v_{j'}) \langle j || Y^{(2)} || j' \rangle \\
 & \times [(a_j^\dagger \tilde{a}_{j'})^{(2)} + c.c.].
 \end{aligned} \quad (10)$$

Here the effective bosonic and fermionic charges are denoted as e_B and e_F and were set equal to the effective bosonic charge, obtained from the respective even-even core.

Given that no experimental data for $M1$ or $E2$ transitions are available in ^{113}Ag , only ^{111}Ag will be considered. In ^{111}Ag , the half-life of the $9/2^+$ state is 1.22 (2) ns and the $9/2^+ \rightarrow 7/2^+$ transition is known to be of a

mixed $M1 + E2$ multipolarity with a mixing ratio of $\delta \leq 0.12$. The experimental $B(M1; 9/2^+ \rightarrow 7/2^+) = 0.024$ W.u. and hence is hindered with respect to the single particle estimates. Since the $E2$ transition strength strongly depends on δ , estimations based on the mixing ratios in the lighter $^{105,107}\text{Ag}$ isotopes were made. They lead to $B(E2) = 120$ (70) W.u. for this particular transition, suggesting that collective modes are involved to a large extent. On the other hand, the hindrance of $B(M1)$ suggests that either $\Delta L = 2$ single-particle orbits are involved, or a more complex configuration exists in the silver spectra at low energies. The only positive parity orbit placed close to the Fermi surface is the intruder $\pi g_{9/2}$ level and, hence, the scenario for l -forbidden transition can be ruled out. Indeed, the structure of the two states, which appear in all neutron mid-shell Ag nuclei, is considered to arise from a $\pi g_{9/2}^{-3}$ configuration. In the seniority scheme framework, however, the $M1$ transition would be forbidden [4], which vaguely agrees with the experimental observable. Even though such three-particle configurations are outside the IBFM-1 model space, it is worth pushing the model to the limit and test it for the two Ag isotopes.

In the present work, the d -boson g -factor $g_d = 0.3 \mu_N$ was determined from the magnetic moment of the first 2^+ state in the neighbouring Cd nuclei [38], where $g_s = 4.0 \mu_N$ and $g_l = 1.0$ were used. By using this value, and the IBFM-1 Hamiltonian parameters deduced from the level energies, we obtain $B(M1; 9/2_1^+ \rightarrow 7/2_1^+) = 0.028$ W.u. which is consistent with the experimental value of 0.024 (1) W.u.. The theoretical calculations show that the $9/2_1^+ \rightarrow 7/2_1^+$ transition has a collective component, with $B(E2) = 27$ W.u., which vaguely agrees with the strength of 120 (70) W.u. estimated from the experimental data. This discrepancy suggests that precise experimental measurement of $M1 + E2$ mixing ratio is needed before making any firm conclusion on the nature of the states involved. Magnetic moments for $7/2^+$ and $9/2^+$ states are calculated and presented in Table VII along with transition strengths for the $9/2_1^+ \rightarrow 7/2_1^+$, $11/2_1^+ \rightarrow 9/2_1^+$ and $13/2_1^+ \rightarrow 9/2_1^+$ transitions. Given that there are no lifetime measurements available for the higher-lying excited states in $^{111,113}\text{Ag}$ only branching ratios can be extracted from the data and used as a reference to the theoretical calculations. They are presented in Table VIII, where a good agreement with the experimental data is observed.

Although the structure of the low-lying states in Ag nuclei is rather complex and involves degrees of freedom that are outside of the present theoretical approach, some conclusions can be drawn from the present work. The core nuclei $^{112,114}\text{Cd}$ are well reproduced by the IBM-1 calculations. Their level schemes are typical for the U(5) nuclei [43], where the relative position of the 0_2^+ with respect to the $2^+, 4^+$ doublet from the second phonon is an indicative feature.

A summary of the strongest single-particle contributions to the wave functions of the lowest-lying states in

TABLE VII: Calculated magnetic moments and transition strengths in $^{111,113}\text{Ag}$.

nucleus	$\mu(7/2^+)$	$\mu(9/2^+)$	$B(M1)$	$B(E2)$	$B(E2)$	$B(E2)$
	μ_N	μ_N	$9/2^+ \rightarrow 7/2^+$	$9/2^+ \rightarrow 7/2^+$	$11/2^+ \rightarrow 9/2^+$	$13/2^+ \rightarrow 9/2^+$
			W.u.	W.u.	W.u.	W.u.
^{111}Ag	4.81	5.90	0.028	27	43	6
^{113}Ag	4.71	5.80	0.018	41	59	5

TABLE VIII: Experimental and Theoretical Branching Ratios in ^{111}Ag and ^{113}Ag .

nucleus	IBFM Exp		
^{111}Ag	$11/2^+ \rightarrow 9/2^+$	100	100.0 (14)
^{111}Ag	$11/2^+ \rightarrow 7/2^+$	0.1	6.0 (8)
^{111}Ag	$13/2^+ \rightarrow 9/2^+$	100	100.0 (17)
^{111}Ag	$13/2^+ \rightarrow 11/2^+$	15.3	5.0 (17)
^{113}Ag	$11/2^+ \rightarrow 9/2^+$	100	100
^{113}Ag	$11/2^+ \rightarrow 7/2^+$	0	0
^{113}Ag	$13/2^+ \rightarrow 9/2^+$	100	100.0
^{113}Ag	$13/2^+ \rightarrow 11/2^+$	12.8	28.5

^{111}Ag and ^{113}Ag is presented in Table IX. The analysis shows that $\pi g_{9/2}$ has a major contribution to the lowest-lying positive-parity states. The leading configuration for the ground states in ^{111}Ag and ^{113}Ag is $\pi p_{1/2}$. This configuration is responsible also for other low-lying negative-parity states, not shown in Fig. 6. At higher energies, however, the $\pi f_{5/2}$ starts to play a role in the structure of the negative-parity states. In particular, this is the case for all negative-parity states with energies above ~ 2 MeV, shown in Fig. 6. All negative parity states with $J^\pi \geq 15/2^-$ have their counterparts in the experimental data. It is interesting to note that the $15/2^-$ band-head energy is well reproduced, but the experimental sequence on top of it shows a more rotational behavior, suggesting that the experimental bands have a quadrupole deformation higher than that of the respective Ag ground state.

IV. CONCLUSIONS

$^{111,113}\text{Ag}$ nuclei were populated in induced fission reactions. The level schemes were extended and the

spin/parities of the new levels are based on systematics. To interpret the structure of the excited states IBFM-1 was used. The ground state in the two nuclei is associated to the $\pi p_{1/2}$ configuration. At higher energies, above 2 MeV, the $\pi f_{5/2}$ configuration starts to play a leading role. Those levels are arranged in band-like sequence, suggesting a deformation, larger than the ground state deformation, is developed there. The positive-parity states are also well described by the model. The $(7/2^+, 9/2^+)$ doublet splitting is correctly reproduced. The $B(M1; 9/2^+ \rightarrow 7/2^+)$ transition rate in ^{111}Ag agree with the experimental observations, while further experimental data on the $M1 + E2$ mixing ratio is needed in order to have a better experimental reference point. However, an overall good agreement with the experimental data is observed, suggesting that the $^{111,113}\text{Ag}$ nuclei exhibit well-developed collective properties.

V. ACKNOWLEDGEMENTS

This work is supported by the Bulgarian National Science Fund under contract number DFNI-E02/6 and by the German BMBF under grant number 06BN109. SK appreciates the number of interesting and constructive discussions with D.Bucurescu regarding the IBFM-1 calculations. SL acknowledges the constructive discussions with P. Van Isacker and V. Paar.

VI. ADDENDUM

While preparing the present manuscript, ^{113}Ag partial level scheme was observed from an experiment performed at GANIL and published in Ref.[44]

-
- | | |
|---|--|
| <p>[1] M. Goepert-Mayer, Phys. Rev 74, 235 (1948); 78, 16 (1949).</p> <p>[2] L.S. Kisslinger, Nucl. Phys. 78, 341 (1966).</p> <p>[3] Kris L.G. Heyde, <i>The Nuclear Shell Model</i>, Springer-Verlag (1994).</p> <p>[4] P. Van Isacker, private communications.</p> <p>[5] L.-G. Svensson, O. Bergman, A. Bäcklin, N.-G. Jonsson, and J. Linkskog, Phys. Scr. 14, 129 (1976).</p> <p>[6] S. Lalkovski, <i>et al</i>, Phys. Rev. C87 034308, (2013).</p> <p>[7] K. Heyde and V. Paar, Phys. Lett. B 179, 1 (1986) and</p> | <p>references therein.</p> <p>[8] A. de Shalit, Phys. Rev. 122, 1530 (1960).</p> <p>[9] V. Paar, Nucl. Phys. A211, 29 (1973).</p> <p>[10] R. Popli, J.A. Grau, S.I. Popik, L.E. Samuelson, F.A. Rickey, and P.C. Simms, Phys. Rev. C20, 1350 (1979).</p> <p>[11] S.Zeghib, F.A. Rickey, and P.C. Simms, Phys. Rev. C34, 1451 (1986).</p> <p>[12] U. Kaup, R. Vorwerk, D. Hippe, H.W. Schuh, P. von Brentano, and O. Scholten, Phys. Lett. B106, 439 (1981).</p> |
|---|--|

TABLE IX: Contributions of different single-particle components to the wave functions of the lowest-lying IBFM-1 states in $^{111,113}\text{Ag}$ nuclei.

^{111}Ag						
J^π	E_{level}^\dagger [keV]	$\pi p_{3/2}$ [%]	$\pi f_{5/2}$ [%]	$\pi p_{1/2}$ [%]	$\pi g_{9/2}$ [%]	$\pi d_{5/2}$ [%]
$1/2^-$	0.0	2.9778	6.3163	90.7059	0.0	0.0
$7/2^+$	60	0.0	0.0	0.0	97.4192	2.5808
$9/2^+$	130	0.0	0.0	0.0	97.9084	2.0916
^{113}Ag						
J^π	E_{level}^\dagger [keV]	$\pi p_{3/2}$ [%]	$\pi f_{5/2}$ [%]	$\pi p_{1/2}$ [%]	$\pi g_{9/2}$ [%]	$\pi d_{5/2}$ [%]
$1/2^-$	0.0	3.6437	7.7439	88.6123	0.0	0.0
$7/2^+$	44	0.0	0.0	0.0	97.2490	2.7510
$9/2^+$	139	0.0	0.0	0.0	97.1381	2.8619

[†]from [38]

- [13] J. Rogowski et al., Phys. Rev. **C42**, 2733 (1990).
 [14] J. Blachot, Nucl. Data Sheets **110**, 1239 (2009).
 [15] J. Blachot, Nucl. Data Sheets **111**, 1471 (2010).
 [16] J. Simpson, Z. Phys. **A358**, 139 (1997).
 [17] D. C. Radford, Nucl. Instr. Meth. A **361**, 297 (1995).
 [18] T. Kutsarova, et al., Phys. Rev. **C79**, 014315 (2009).
 [19] S. Lalkovski, et al., Phys. Rev. **C 75**, 014314 (2007).
 [20] E. A. Stefanova, et al, Phys. Rev. **C86**, 044302, (2012).
 [21] S. Lalkovski, et al, Phys. Rev. **C89**, 064312, (2014).
 [22] D.E. Brown, K.S. Krane, Nucl.Phys. **A489**, 100 (1988).
 [23] R.E. Anderson, J.J. Kraushaar, I.C. Oelrich, R.M. DelVecchio, R.A. Naumann, E.R. Flynn, C.E. Moss, Phys. Rev. **C15**, 123 (1977).
 [24] R.E. Anderson, J.J. Kraushaar, R.A. Emigh, P.A. Batay-Csorba, H.P. Blok, Nucl.Phys. **A287**, 265 (1977).
 [25] S. Zeghib, F.A. Rickey,, G.S. Samudra, P.C. Simms, and N. Wang, Phys. Rev. **C36**, 939 (1987).
 [26] S.Y. Van der Werf, B.Fryszczyn, L.W.Put, R.H.Siemssen, Nucl.Phys. **A273**, 15 (1976).
 [27] F. R. Espinoza-Quinones, et al., Phys. Rev. **C55**, 1548 (1997).
 [28] F. Iachello and O. Scholten, Phys. Rev. Lett. **43**, 679 (1979).
 [29] F. Iachello and P. Van Isacker, The Interacting Boson-Fermion Model, Cambridge University Press (1991).
 [30] F. Iachello and A. Arima, Physics Letters B **53**, 309 (1974).
 [31] A. Arima and F. Iachello, Phys. Rev. Lett. **35**, 1069 (1975).
 [32] R. F. Casten and D. D. Warner, Rev. Mod. Phys. **60**, 389 (1988).
 [33] W. Pfeifer, An Introduction to the Interacting Boson Model of the Atomic Nucleus, vdf-Hochschulverlag AG an der ETH Zürich (1998).
 [34] D. Bucurescu, G. Căta, D. Cutoiu, G. Constantinescu, M. Ivaşcu, and N.V. Zamfir, Z. Phys. A **324**, 387 (1986).
 [35] P. O. Lipas, P. Toivonen, and D. D. Warner, Phys. Lett. B **155**, 295 (1985).
 [36] R. F. Casten, *Nuclear Structure from a Simple Perspective* (Oxford University Press, Oxford, 1990)
 [37] O. Scholten, the program package PHINT, internal report KVI-63, Kernfysisch Versneller Instituut, Groningen, The Netherlands.
 [38] NNDC data base (www.nndc.bnl.gov).
 [39] J. Jolie, P. Van Isacker, K. Heyde, J. Moreau, G. Van Landeghem, M. Waroquier, and O. Scholten, Nuclear Physics A **438**, 15 (1985).
 [40] O. Scholten, Ph. D. thesis, University of Groningen (1980).
 [41] O. Scholten, program package ODDA, KVI internal report no. 255 (1980).
 [42] B. S. Reehal and R. A. Sorensen, Phys. Rev. C **2**, 819 (1970).
 [43] D. Bonatsos, Interacting Boson Models of Nuclear Structure, Clarendon Press, Oxford (1988).
 [44] Y. H. Kim et al, Phys. Lett. **B772**, 403 (2017)